MethodsX 10 (2023) 101955

Contents lists available at ScienceDirect

MethodsX

journal homepage: www.elsevier.com/locate/mex

Method Article

Clay exfoliation method as a route to obtain mesoporous catalysts for CO_2 methanation ☆,☆☆

Daniel Cortés-Murillo, Carolina Blanco-Jiménez, Carlos E. Daza*

Estado Sólido y Catálisis Ambiental, Departamento de Química, Facultad de Ciencias, Universidad Nacional de Colombia, Sede Bogotá, Bogotá, D.C., Colombia

ARTICLE INFO

Method name:
Microwave-assisted clay exfoliation

Keywords:
Climate change
Synthetic natural gas
Exfoliated clay
Mesoporous materials

ABSTRACT

A unique method for obtaining a mesoporous catalytic support through the exfoliation of a montmorillonite is reported. This method consisted of the intercalation of Na-clay with Al-Keggin species and polyvinyl alcohol followed by microwave irradiation. The mesoporous support was employed to prepare Ni-catalysts which were used in the natural gas synthesis through CO_2 methanation. The synthesis method was validated confirming the clay exfoliation and the main formation of mesopores. Also, the Ni-catalysts have mainly weak basic surface properties lower than 38 $\mu mol.g^{-1}$, and containing Ni^0 nanoparticles with sizes between 9 and 12 nm which were thermally stable after reduction and methanation reaction. The catalyst with 5% Ni wt. gave conversions between 50 and 80% with temperatures ranging from 200 to 300 °C and selectivities of 100% towards the formation of CH_4 without coke formation. The (3 and 5% Ni) Ni-catalysts are stable up to 8 h at 400 °C in the methanation reaction maintaining 100% of selectivity.

- Mesoporous catalytic supports are obtained through a unique clay exfoliation method (Al-keggin, PVA, and microwaves).
- (3% and 5% wt.) Ni-mesoporous catalysts are thermally stable and Ni^0 nanoparticles between 9 and 12 nm are achieved.
- 5%wt. Ni-catalyst have no deactivation up to 8 h at 400 °C and displays unprecedented performance at low temperatures in CO_2-methanation with 100% of selectivity.

☆ Related research article C. Daza, A. Kiennemann, S. Moreno, R. Molina, Dry reforming of methane using Ni–Ce catalysts supported on a modified mineral clay, Appl. Catal. A Gen. 364 (2009) 65–74. doi:10.1021/ef9000874.

☆☆ C. Daza, A. Kiennemann, S. Moreno, R. Molina, Stability of Ni-Ce catalysts supported over Al-PVA modified mineral clay in dry reforming of methane, Energy and Fuels. 23 (2009) 3497–3509. doi:10.1021/ef9000874.

* Corresponding author.
E-mail address: cedazav@unal.edu.co (C.E. Daza).

https://doi.org/10.1016/j.mex.2022.101955
Received 8 September 2022; Accepted 29 November 2022
Available online 2 December 2022
2215-0161/© 2022 The Author(s). Published by Elsevier B.V. This is an open access article under the CC BY-NC-ND license (http://creativecommons.org/licenses/by-nc-nd/4.0/)

Specifications table

Subject area	Materials Science
More specific subject area	Heterogeneous Catalysis
Name of your method	Microwave-assisted clay exfoliation
Name and reference of original method	C. Daza, A. Kiennemann, S. Moreno, R. Molina, Dry reforming of methane using Ni–Ce catalysts supported on a modified mineral clay, Appl. Catal. A Gen. 364 (2009) 65–74. doi:10.1021/ef9000874. C. Daza, A. Kiennemann, S. Moreno, R. Molina, Stability of Ni-Ce catalysts supported over Al-PVA modified mineral clay in dry reforming of methane, Energy and Fuels. 23 (2009) 3497–3509. doi:10.1021/ef9000874.
Resource availability	N.A.

Method details

Background

Industrialization and technological advances have caused global energy consumption to double in the last 20 years [1]. As a consequence of human activities, such as the consumption of fossil fuels, a huge amount of CO_2 is emitted, which is one of the greenhouse gases responsible for climate change. Liu Z. et al. [2] reported that annual worldwide CO_2 emissions increased from 33.3 $GtCO_2$ in 2020 up to 34.9 $GtCO_2$ in 2021, which corresponds to a 4.8% increase. CO_2 methanation has received great interest because it has the potential to reduce anthropogenic CO_2 emissions through its catalytic transformation into CH_4 better known as synthetic natural gas (SNG) which is a product of exceptional commercial value as a fuel [3]. The methanation reaction is industrially viable to obtain SNG sustainably since the reaction consumes green hydrogen and CO_2 captured from the atmosphere.

At present, the study and development of catalysts for CO_2 methanation thermally stable and highly active at low temperatures is a great challenge [4]. The viability of a catalyst is determined by different properties such as stability, cost, and selectivity. Methanation has been investigated using several Ni-based catalyst systems on different oxide-type supports. The surface chemistry, textural parameter, and morphology of the support play a crucial role in the interaction between Ni and the support and thus determine the activity and selectivity parameters [5]. Certain types of supports could improve some catalytic properties such as metal phase reduction, active metal dispersion, and mechanical and thermal stability.

Clay minerals have been widely employed in numerous catalytic processes, including some work on CO_2 methanation, which are excellent candidates as catalytic supports [6,7]. Clays are materials of a crescent industrial interest because of their great abundance and low cost. The porosity and surface chemical properties of clays can be modified through methods of modifying their interlayer space [8]. For example, the introduction of Al-polycations (pillarization method) generates materials with high thermal stability. In addition, clay exfoliation methodologies where the presence of surfactants during the intercalation step is involved, have been proposed as an alternative to pillarization method [9]. The interactions and stacking of the clay layers can be modulated by the presence of surfactants, obtaining an exfoliated structure with thermal stability up to 700 °C, and the presence of mesopores and macropores [10]. Mesoporous materials can enhance the available area for the nanoparticle deposition of the active phase, promote diffusive processes of the reactants and avoid carbon accumulation, this is particularly important in sensitive reactions to particle size as CO_2 methanation [11]. Recently, the critical review developed by Keen Fan W. and Tahir M. [12], systematically gathered the applications of various structured and modified clay minerals-based nanomaterials for CO_2 hydrogenation reactions concluding that clays are materials that show promising features as catalysts for the methanation reaction.

In this work, we detail our previously reported method for the exfoliation of montmorillonites using Al polycations, a surfactant (polyvinyl alcohol), and microwaves to achieve thermally stable mesoporous support for Ni catalysts [13,14]. The method here reported consists of an rapid and reproducible methodology with easy-to-handle and low-emission reagents involving a highly available low-cost or no-cost material. Clays are minerals with different characteristics depending on the geographical location from which minerals are extracted, so the method is useful to obtain a wide range of mesoporous solids that are characterized by high thermal and chemical stability. In our previous research, the promoted Ni-Ce catalysts performed well in the dry reforming of methane, and the mesoporosity improved the distribution of active phases and avoided coke accumulation and thus decreased catalyst deactivation [13,14]. For these reasons, the exfoliation method can be used to obtain catalysts with different active phases and use them in reactions where mesoporosity can have beneficial effects on performance.

We describe the characterization (crystalline and chemical composition, morphology, crystallite, Ni^0-particle sizes and basicity) of the support and the Ni catalysts (3 and 5%wt.). Besides, we show the catalytic tests in the CO_2 methanation reaction to validate the method as a way to produce catalysts with good catalytic performance in the reaction.

Method description

Chemicals

NaCl (Panreac®, 99%wt.), $Al(NO_3)_3.9H_2O$ (Panreac®, 99%wt.), NaOH (Panreac®, 99%wt.) polyvinyl alcohol (PVA) (M_w 89,000-98,000, Alfa Aesar®, 98%wt.), and $Ni(NO_3)_2.6H_2O$ (Panreac®, 98%wt.).

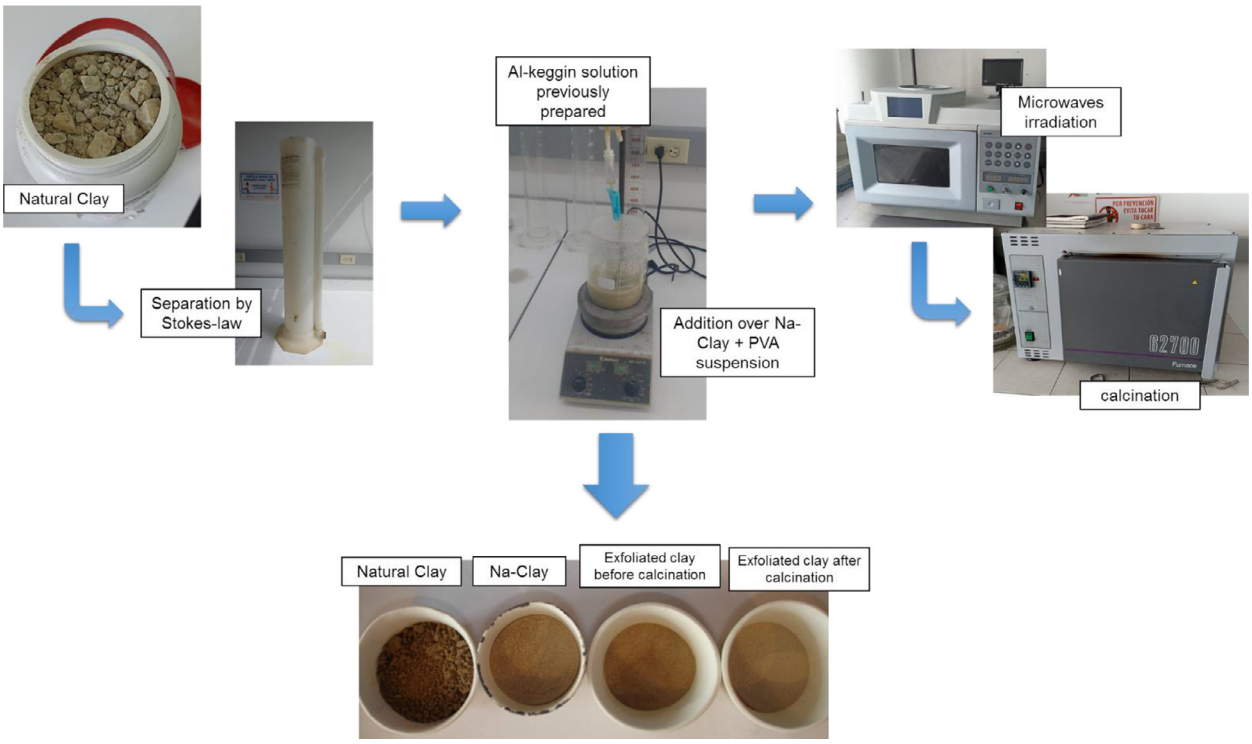

Fig. 1. Step by step of clay exfoliation method.

The clay was a montmorillonite-type from Colombia with a 62% of smectite phase. The elemental composition of clay by X-ray fluorescence is 59.38 ± 0.03%wt SiO_2, 15.59 ± 0.02%wt. Al_2O_3, 6.68 ± 0.01%wt. Fe_2O_3, 3.04 ± 0.02%wt. MgO, and 2.68 ± 0.02%wt. CaO.

Na-saturation of the clay

The natural mineral was crushed and the particle size fraction less than 50 μm was separated using Stokes' Law. 100 g of the clay were dispersed in 10 L of water using a tube 1 m long and 20 cm in diameter. The mixture was vigorously shaken and after 20 s, the upper 20 cm of the suspension was removed and dried at 100 ˚C. The dry material was crushed and sieved with a 150 μm mesh. Subsequently, the mineral was dispersed at 5% w/v in a 10% w/v solution of NaCl, left stirring for 24 h, and separated by centrifugation. The process was repeated twice. Finally, the solid was washed until free of chlorides, separated by centrifugation, dried at 100 ˚C for 24 h, crushed, and sieved with a 150 μm mesh.

Preparation of the Al-Keggin solution

0.5 M solutions of aluminum nitrate and sodium hydroxide were prepared. Then, 800 mL of NaOH solution was added dropwise to 400 mL of Al^{3+} solution at 60 ˚C, these quantities are enough to reach a molar ratio of OH^-/Al^{3+}=2. The addition should be slow (drop by drop) and under vigorous stirring to avoid the formation of a hydroxide precipitate. Finally, the solution was aged for 24 h at room temperature and stored.

Clay exfoliation

The Na-clay (10 g) was dispersed at 2% w/v in water and allowed to swell for 24 h. Simultaneously, a PVA colloidal dispersion was prepared using 20 g of PVA in 250 mL of water at 80 ˚C. This dispersion was added slowly to the clay suspension at 80 ˚C. After one hour, the Al-Keggin solution (1200 mL) was added dropwise to the PVA-clay suspension (20 mmol Al^{3+}/g_{clay}). The suspension was aged for 24 h at 60 ˚C under vigorous stirring. Finally, the slurry was irradiated with microwaves (640 W and 2.45 GHz) in three intervals of 10 min. This irradiation should not be done continuously to avoid overheating and possible splashes. The mixture was decanted and dried at 80 ˚C. The resulting material was calcined at 500 ˚C for 4 h with a ramp of 2˚C/min, slow enough to avoid destroying the porosity of the material. Fig. 1 shows detailed images of the step by step of clay exfoliation method.

Table 1
Characterization of exfoliated clay and catalysts.

Solid	% wt. Ni*	Ni° crystallite size (nm)**	B.E.T. surface (m^2g^{-1})	Mesopores surface (m^2g^{-1})	Reducibility (%)	CO_2-uptake (μmol/g) by TPD
Na-Clay	-	-	34	13	-	-
Exfoliated clay	-	-	142	127	88.4	50 ± 5
3% Ni	3.10 ± 0.02	6.2	106	93	74.5	38 ± 5
5% Ni	5.30 ± 0.02	12.2	89	77	75.6	22 ± 5

* The elemental analysis by XRF confirmed the Ni-loads in the catalysts.
** Calculated by Scherrer's method from XRD of reduced samples.

Preparation of Ni catalysts

The incipient impregnation technique followed by ultrasound was used for the preparation of the Ni-catalysts. $Ni(NO_3)_2.6H_2O$ was employed as precursor salt. 1 g of the support was impregnated with 10 mL of solutions containing 3 and 5 wt% Ni followed by 30 min of ultrasound. The solids were dried overnight at 80 °C and calcined at 500 °C for 4 h using a ramp of 10°C/min.

Characterization techniques

The elemental analysis was carried out by X-Ray Fluorescence (XRF), on a MagixPro PW-2440 Phillips® spectrometer. X-Ray Diffraction (XRD) profiles were measured in a Panalytical® XPert PRO MPD using a Cu-anode and a step size of 0.02 $^{\circ}2\theta.s^{-1}$. Ni° crystallite sizes were calculated using Scherrer's equation. N_2-adsorption isotherms at 77 K were obtained in Micromeritics® ASAP2020 equipment previous degassing at 300 °C for 4 h. The temperature-programmed reduction (H_2-TPR) profiles and reducibility were measured using Chembet3000 Quantachrome® equipment coupled with a thermal conductivity detector (TCD) according to methodologies reported elsewhere [15]. CO_2-uptake measurements and CO_2-Temperature Programmed Desorption of (CO_2-TPD) profiles were performed using a Chembet 3000 Quantachrome® device; 100 mg of catalyst was pre-treated in He at 500 °C for 1 h and cooled to 25°C before pulses adsorption, 100 μL pulses of pure CO_2 were injected until total saturation and desorption was made under He flow at 10°C.min^{-1} and measured with the TCD detector. Scanning Electron Microscopy (SEM) images were taken with a Fei-Quanta® 200 microscope.

The average Ni^0 diameter particle size distributions of the catalysts pre-reduced at 600 °C were determined by transmission electron microscopy (TEM) using a JEOL® JEM-1400 Plus equipment coupled to Energy Dispersive X-Ray Analyzer (EDX).

CO_2 Methanation tests

The catalytic tests were carried out using a microreactor set-up equipped with a 6 mm internal diameter quartz reactor, the detailed reaction set-up can be seen in Fig. 1S (supplementary materials). The catalyst was mixed with SiC and packed into a 10 mm long catalyst bed. The reduction of the catalyst was made *in situ* for 1 h under H_2 at 30 mL.min^{-1} at 600 °C (selected according to the results of H_2-TPR). Subsequently, the reactor was fed with a mixture of CO_2/H_2/He 10/40/50%vol. at 50 mL.min^{-1} and WHSV = 52400 mL.$(g.h)^{-1}$. Catalytic tests as a function of reaction temperature and stability tests at 400 °C (for 8 h) were performed. The steady-state reactants and products were measured online with an Agilent® 7890A gas chromatograph (GC), composed of two detectors (TCD+FID), and two columns (HP-PLOT molecular sieve and HP-PLOT U). Detailed methodology for GC measurements can be found in Table 1S (supplementary materials). Additionally, the equations to calculate % CO_2-conversion and% CH_4-selectivity are shown in the supplementary materials.

After the reaction, the materials were characterized through thermo-gravimetry analysis (TGA) and differential scanning calorimetry (DSC) under air atmosphere to quantify the coke formation, using the microbalance of TA SDT® Q 600 equipment.

Method validation

Fig. 2 shows a comparison between the XRD profiles of the Na-clay and the exfoliated clay. The Na-clay XRD exhibits signals corresponding to typical phases existing in natural minerals (feldspar+quartz+illite) and the 001 (*hkl*) signal corresponding to the T:O:T stacking of the smectites with a value d = 1.46 nm agreeing to montmorillonite-type phase [16]. The XRD signals of the feldspar+quartz+illite phases remained unchanged after the exfoliation methodology, however, the 001 (*hkl*) signal showed a decline in intensity and a shift towards a value of d = 1.85 nm, indicating that the methodology-induced alterations in the stacking of the smectite layers. Indeed, the loss of intensity suggests the damage to the layers' crystallinity caused by exfoliation, and the occurrence of low-intensity signals shifted towards d = 1.85 nm implies the presence of fragmentsof Al-pillared layers [10].

The N_2 adsorption isotherms of Na-clay and exfoliated clay were type IV (hysteresis H3) consistent with mesoporous solids (see Fig. 2S in supplementary materials). The 3% Ni catalyst presented a more extensive H3-type hysteresis close to the H2-type, which indicates the formation of pores with greater heterogeneity. The textural parameters listed in Table 1 show both an increase in the B.E.T area as well as in the mesopores area of the Na-clay after exfoliation. Beside, an increase in the ratio of mesopores area vs B.E.T area was observed after exfoliation, revealing the higher proportion of mesopores vs micropores in the catalytic support.

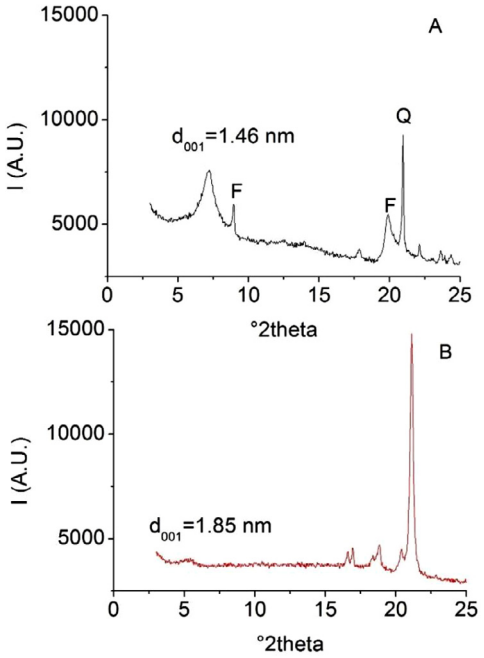

Fig. 2. Powder XRD for A. Natural Na-clay and B. Exfoliated clay.

The mostly mesoporous character of the exfoliated clay was confirmed by the monomodal distribution of pore sizes (B.J.H model) with a maximum of 28 nm vs 0.5 nm for Na-clay. The modification of the clay porosity was effective, and it mainly occurred for the exfoliation of the clay layers. These results are in agreement with those reported which indicate that exfoliation produces a mostly mesoporous solid, while pillarization generates a predominantly microporous solid [17].

After the Ni impregnation (3% and 5% wt.), there was a decrease in the B.E.T area vs catalytic support (exfoliated clay) (see Table 1) caused by the formation of NiO particles blocking the pores. In addition, an increase in Ni load caused a decrease in the B.E.T area (106 m^2g^{-1} vs 89 m^2g^{-1}, respectively) and the mesopore area (93 m^2g^{-1} vs 77 m^2g^{-1}, respectively). However, the catalysts maintained the mainly mesoporous character since the mesoporous areas matched to 88–90% of the total area, and the pore size distributions exhibited maximums between 20 and 30 nm.

The XRD of the catalysts (see Fig. 3A) did not present a signal close to 10 °2θ suggesting structural reorganization or collapse of the layered structure after impregnation and calcination, therefore, the modification with Al gave thermal stability to the material. The XRD of the catalysts showed characteristic signals of the NiO phase with low intensity, which indicated good dispersion of the metal in the support. The NiO crystallites provided sizes of 12 nm and 18 nm for the 3% and 5% catalysts, respectively.

Fig. 3B depicts the H_2-TPR profiles of the support and the NiO phase contained in the catalysts. The exfoliated clay H_2-TPR revealed a reduction peak at 670 °C probably corresponding to the reduction of FeO (wustite phase) to Fe^0 and a low-intensity peak at 485°C assigned to the reduction of Fe_2O_3 (hematite phase) to Fe_3O_4 (magnetite phase) [18]. The H_2-TPR for Ni-catalysts showed the main reduction signal at 520-530 °C consistent with the reduction of highly interacting NiO species probably located in the pores of the catalytic support and at the edges of the clay layers [14]. Only the catalyst with 5% wt. Ni showed a reduction signal at 335 °C according to low-interacting NiO formed by oxide multilayers accumulated when the Ni charge increases.

The (%) reducibility indicated that only 88.4% of the total Fe in the material can be reduced and 75% (approx.) of the Ni impregnated in both catalysts can be reduced to form Ni^0 species (see Table 1). Thus, after H_2-TPR analysis the reduction temperature selected was 600°C which is enough to reduce all NiO and partially Fe^{3+} to Fe^{2+}.

The XRD for the reduced catalysts (see Fig. 3C) did not show alterations of the material structure, loss of crystallinity, or collapse of the clay structure after reduction at 600 °C. XRD Ni^0-signals and persistent NiO-signals were observed which is in agreement with the calculated reducibilities. The crystallite sizes (see Table 1) of Ni° for reduced samples at 600 °C were 6.2 and 12.2 nm for the 3% and 5% wt. catalysts, respectively. As expected, an increase in crystallite size with an increase in Ni loading was obtained. In addition, Ni^0 particle sizes were confirmed with TEM images coupled to EDX chemical analysis (see Fig. 4) revealing a monomodal size distribution for mostly spherical particles with average sizes at 9.6 ± 3.0 nm for the 3%wt. Ni and 12.1 ± 4.2 nm for the 5%wt. Ni. The results of the crystallite size by Scherrer's method and the TEM particle size distribution maximums were consistent with each other.

Fig. 3E illustrates CO_2-TPD profiles and Table 1 shows the CO_2-uptake as a direct measure of the solids basicity determined by pulse chemisorption. The profiles show typical CO_2-TPD of a solid of low basicity or mainly weak basic properties showing low signal intensities compared to basic solids used in CO_2 methanation and the absence of signals at temperatures above 400 °C indicating the

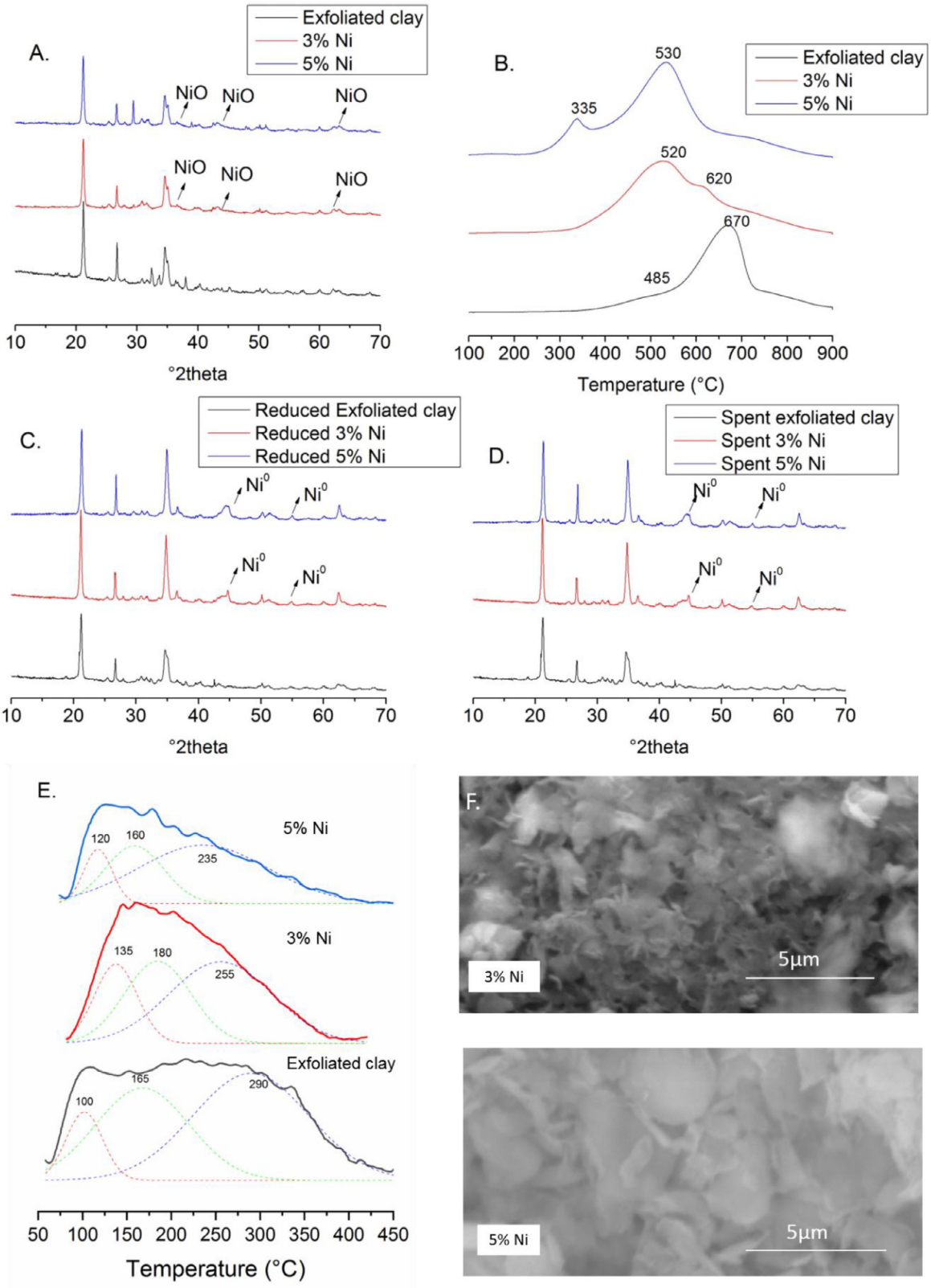

Fig. 3. A. XRD for catalysts, B. H_2-TPR, C. XRD for reduced catalysts at 600°C, D. XRD for spent catalysts, E. CO_2-TPD, and selected SEM images for catalysts.

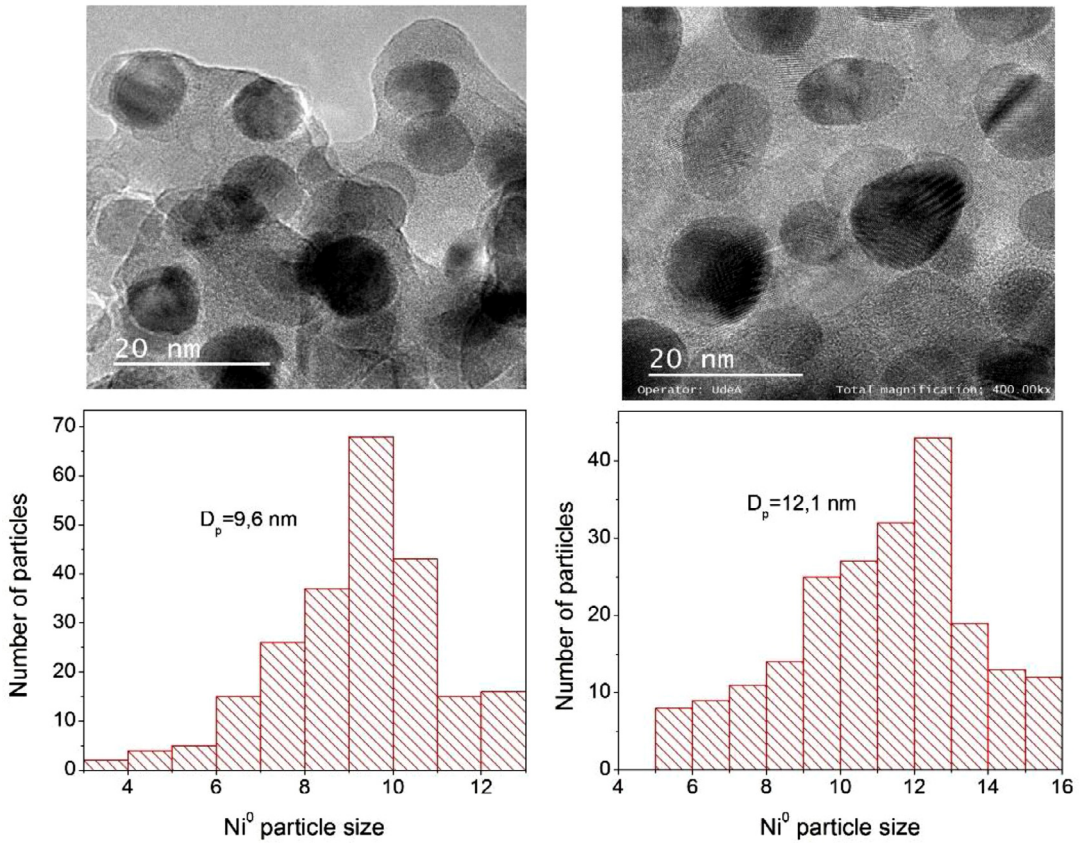

Fig. 4. TEM selected images and Ni^0 particle distributions for (left) 3% Ni and (right) 5% Ni.

formation of carbonates with high thermal stability. The total basicity of the catalytic support was 50 ± 5 μmol.g^{-1} and of the 3 and 5% Ni-catalysts was 38 ± 5 and 22 ± 5 μmol.g^{-1}, respectively, which are lower than those reported, for example, by Yang x. et al. [19] between 115 and 220 μmol.g^{-1} for basic Ni-Mg-Al oxides with different compositions, by Rien J. et al. [20] which were between 89 and 133 μmol.g^{-1} for Ni oxides derived from hydrotalcites, or significantly lower than those reported by Li Y. et al [21] between 290 and 790 μmol.g^{-1} for Ni-supported on natural palygorskite-clay.

The mathematical deconvolution of the CO_2-TPD signals generated three peaks that, according to the literature, can be classified as sites of weak (100-135 °C), medium (160-180 °C), and strong basicity (235-290 °C). The sites of weak basicity may correspond to surface sites where physisorption occurred mainly, while the sites of weak and strong basicity may correspond to terminal hydroxyls of phyllosilicates where hydroxy-carbonates can be formed, or because of the formation of carbonates with alkaline elements that can be present in the clay [22]. On the other hand, natural Na-clay does not present measurable basicity, so the exfoliation of the clay increases the basicity of the material since it increases the surface area and exposes possibly basic sites [14]. A higher proportion of strong basicity sites (290 °C) was observed in the exfoliated clay (support) compared to the catalysts and a decrease in the total basicity of the catalyst was registered when Ni loading is increased, this indicated that the formation of metallic particles on the catalyst blocked basic sites of the support and that Ni^0 particles do not provide basicity to the solid.

Fig. 3E shows selected SEM images for the Ni-catalysts. The morphology of the catalysts was flakes-like, typical of natural or modified clays [9]. The images did not show the accumulation of Ni granules, which was corroborated by EDX showing a homogeneous distribution of Ni. Additionally, the thermal treatment for the preparation of the Ni-catalysts not destroyed the typical morphology of the exfoliated clay.

Fig. 5 describes both the CO_2 conversion and the selectivity plots of the reaction. The exfoliated clay is not active in the methanation reaction, suggesting that structural Fe in the clay is not enough for the reaction. The increase in conversion for exfoliated clay up to 12% conversion at 500 °C may be due to CO_2 adsorption, which is confirmed by the low selectivity obtained. On the contrary, the Ni-catalysts were active and the results reached thermodynamic equilibrium at 500°C, registering an increase in the conversion with the increase in Ni loading. Between 200 and 300 °C, the catalyst with 3% wt. Ni allowed conversions between 15 and 20% while the catalyst with 5% wt. Ni gave conversions ranging from 50 to 80%. The catalysts were 100% selective towards CH_4 at temperatures below 300 °C and displayed a decrease to 80% for the 3%wt which is agree with thermodynamics. Ni and 85% for the 5%wt Ni at 500°C which agrees with the thermodynamics of the reaction. No coke formation over the catalysts was confirmed by TGA and the catalytic reaction did not cause structural alterations in the solid or Ni° crystallite sizes sintering (see Fig. 3D).

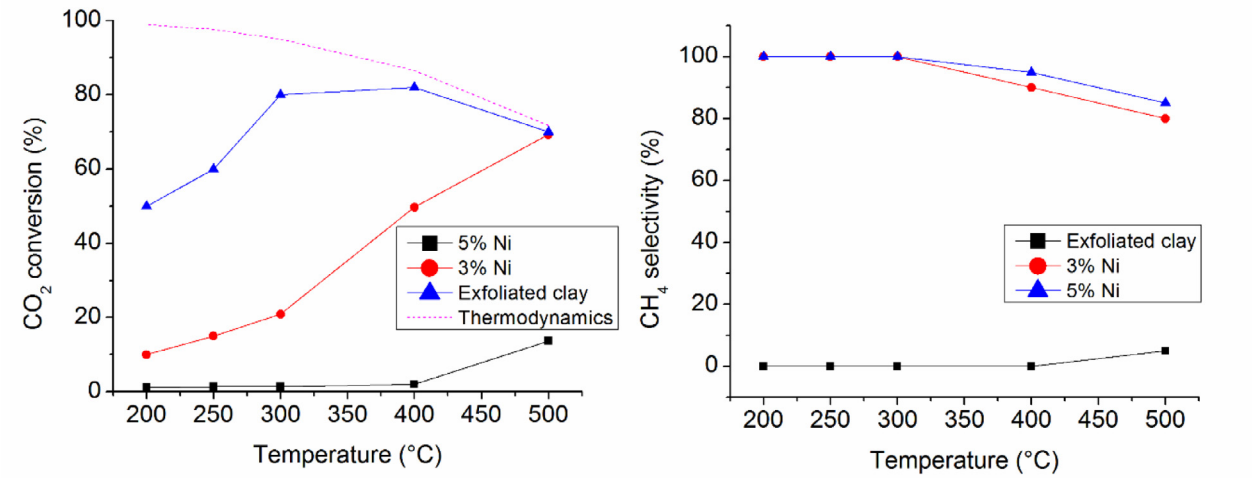

Fig. 5. CO_2 conversions and CH_4 selectivity in the CO_2 methanation reaction. CO_2/H_2/He 10/40/50%vol. and WHSV=52400 mL.(g.h)$^{-1}$

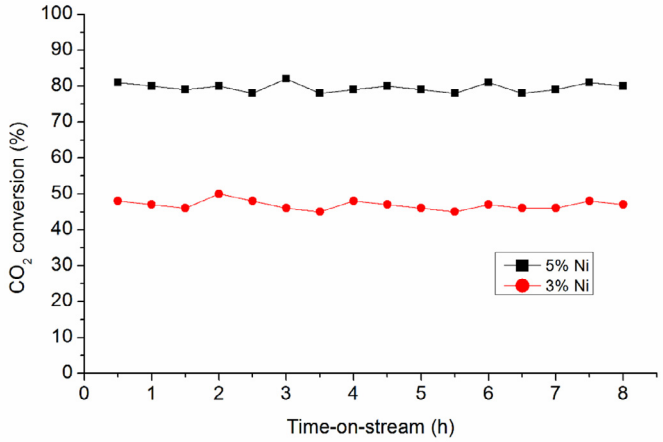

Fig. 6. Stability tests for catalysts at 400°C. CO_2/H_2/He 10/40/50%vol. and WHSV=52400 mL.(g.h)$^{-1}$

The 5% wt. Ni-catalyst reported in this work afforded a very good performance in the CO_2 methanation reaction reaching higher conversions at temperatures between 200 and 250 °C than similar Ni-catalysts supported on clay minerals reported elsewhere. These results are relevant considering that, in comparison, higher space velocities were used in our work. For instance, Lu H. et al. [23] synthesized 15% wt. Ni-catalysts supported on a Volkonskoite (smectite-type clay) and modified with ZrO_2. The catalytic conversions of CO_2 were lower than 40% at 300 °C and 80-82% at 390 °C, while the selectivity to CH_4 was lower than 90% at 300 °C. Also, Lu X. et al. [6] reported Ni-catalysts and VOx-promoted and supported on a bentonite and an acid-alkali-treated bentonite. The catalytic tests in the CO_2 methanation were carried out at 30,000 mL.(g.h)$^{-1}$ showing conversions lower than 40% below 350°C. The 3% wt. VOx-promoted catalyst achieved conversions close to 60-75% between 320 and 360 °C. The best catalysts exhibited a selectivity of 100% at temperatures below 400 °C. Kontchouo et al. [24] tested Ni/clay catalyst supported over clays calcined at several temperatures. The 7.5% and 15% wt. Ni-catalysts provided conversions lower than 40%, being those calcined at 600°C the catalysts that reached the best performance. Lu. H et al. [7] reported metal-doped (La, Ce, Fe, or Co) Ni-catalysts supported on ZrO_2-modified clays followed by the impregnation method. The catalysts registered conversions below 30% at 350 °C. The no-doped catalyst metal gave 71% conversion at 350 °C.

Furthermore, Jiang et al. [25] reported a 20 wt.% Ni/bentonite catalyst synthesized by a solution combustion method which exhibited higher activity for the CO_2 methanation vs the impregnation method. The catalysts were tested at 3600 mL.(g.h)$^{-1}$ and 7200 mL.(g.h)$^{-1}$, obtaining conversions between 70 and 85% at 300 °C, and conversions of less than 45% below 250 °C. In another study, Jiang et al. [26] reported a Ni-catalyst supported by bentonite was promoted with 2 wt.% Mn. Mn created more oxygen vacancies enhancing the CO_2 conversion to CH_4. The catalysts allowed conversions close to 80% at 300 °C, lower than 50% at 250 °C, and lower than 25% at 200 °C. Finally, Liang et al. [27] reported Ni/attapulgite catalysts where the Ni loading varied from 5% to 25% wt. The catalysts were probed at GHSV=16,000 h^{-1} and the conversions were lower than 40% at 300 °C and less than 25% below 250 °C.

The results indicated that the catalytic performance is not related to the greater basicity, the smaller particle size, or the smaller mesopore area that the catalyst with 3% Ni presented concerning the catalyst with 5% Ni, but rather that for these catalysts with the contents of Ni evaluated, a greater number of Ni active sites available is better.

Fig. 6 shows stability tests for the (3 and 5%) Ni-catalysts, which indicated that the catalysts do not present deactivation and that the conversion values remain at 80 ± 3% for the 5% Ni catalyst and at 50 ± 3% for the 3% Ni catalyst, consistent with the tests as a function of reaction temperature. The TGA-DSC of the catalysts used in the stability tests are presented in Fig. 3S (supplementary materials), which showed only two events; the first was an endothermic event between 100 and 120°C corresponding to the loss of physisorbed water and CO_2 (5% wt. approximately), and the second was an endothermic event at 600°C which may be due to loss of surface carbonate species (1-2% wt. approximately). However, no exothermic events were recorded to corroborate the coke formation on the catalyst surface.

On the other hand, the selectivity of the stability tests was 100% towards CH_4 since the formation of CO through the reverse of the water-gas shift reaction was not observed, even though the catalytic support contains Fe_2O_3 which can catalyze this reaction [28]. As an example, the chromatograms obtained after 8 h of reaction in the stability tests were included (see Fig. 4S, supplementary materials), which qualitatively demonstrated the non-formation of CO during the reaction.

Conclusion

Our previously reported method to obtain mesoporous catalytic support for Ni, from the exfoliation of a smectite-type clay consisting of PVA, Al-keggin, and microwaves was detailed and validated. Novel Ni-catalysts were prepared, characterized, and tested in CO_2-methanation. The catalysts are mesoporous, thermally stable, and contain Ni^0 nanoparticles between 9 and 12 nm. The Ni catalyst with 5% wt. shows an unprecedented performance in the CO_2-methanation compared to similar systems at temperatures below 300°C, being selective to the formation of CH_4 and without coke formation. The catalysts are stable up to 8 h at 400 °C maintaining 100% selectivity towards CH_4 formation.

Declaration of Competing Interest

The authors declare that they have no known competing financial interests or personal relationships that could have appeared to influence the work reported in this paper.

CRediT authorship contribution statement

Daniel Cortés-Murillo: Conceptualization, Methodology, Investigation, Validation, Writing – original draft. **Carolina Blanco-Jiménez:** Conceptualization, Investigation, Writing – original draft, Writing – review & editing. **Carlos E. Daza:** Conceptualization, Investigation, Writing – original draft, Writing – review & editing.

Data availability

Data will be made available on request.

Acknowledgments

This work was partially supported by the Universidad Nacional de Colombia [Project number 48248].

Supplementary materials

Supplementary material associated with this article can be found, in the online version, at doi:10.1016/j.mex.2022.101955.

References

[1] A.G. Olabi, M. Ali, Renewable energy and climate change, Renew. Sustain. Energy Rev. 158 (2022) 112111, doi:10.1016/j.rser.2022.112111.
[2] Z. Deng, S.J. Davis, Monitoring global carbon emissions, Nat. Rev. Earth Environ. 3 (2022) 217–219, doi:10.1038/s43017-022-00285-w.
[3] Z. Wang, L. Wang, Y. Cui, Y. Xing, W. Su, Research on nickel-based catalysts for carbon dioxide methanation combined with literature measurement, J. CO_2 Util. 63 (2022) 102117, doi:10.1016/j.jcou.2022.102117.
[4] Q. Zhang, R. Xu, N. Liu, C. Dai, G. Yu, N. Wang, B. Chen, *In situ* Ce-doped catalyst derived from NiCeAl-LDHs with enhanced low-temperature performance for CO_2 methanation, Appl. Surf. Sci. 579 (2022) 152204, doi:10.1016/j.apsusc.2021.152204.
[5] X. Gao, Z. Wang, Q. Huang, M. Jiang, S. Askari, N. Dewangan, S. Kawi, State-of-art modifications of heterogeneous catalysts for CO_2 methanation – Active sites, surface basicity and oxygen defects, Catal. Today 402 (2022) 88–103, doi:10.1016/j.cattod.2022.03.017.
[6] X. Lu, F. Gu, Q. Liu, J. Gao, Y. Liu, H. Li, L. Jia, G. Xu, Z. Zhong, F. Su, VOx promoted Ni catalysts supported on the modi fi ed bentonite for CO and CO_2 methanation, Fuel Process. Technol. 135 (2015) 34–46, doi:10.1016/j.fuproc.2014.10.009.
[7] H. Lu, X. Yang, G. Gao, J. Wang, C. Han, X. Liang, C. Li, Y. Li, W. Zhang, X. Chen, Metal (Fe, Co, Ce or La) doped nickel catalyst supported on ZrO_2 modified mesoporous clays for CO and CO2 methanation, Fuel 183 (2016) 335–344, doi:10.1016/j.fuel.2016.06.084.
[8] J. Moma, Synthesis and application of pillared clay heterogeneous catalysts for wastewater treatment : a review, RSC Adv. (2018) 5197–5211, doi:10.1039/c7ra12924f.
[9] C. Belver, P. Aranda, New silica /alumina – clay heterostructures : properties as acid catalysts, Microporous Mesoporous Mater. 147 (2012) 157–166, doi:10.1016/j.micromeso.2011.05.037.

[10] C. Daza, O. Gamba, Y. Hernandez, M.A. Centeno, F. Mondragón, S. Moreno, R. Molina, High-stable mesoporous Ni-Ce/Clay catalysts for syngas production, Catal. Lett. 141 (2011) 1037–1046, doi:10.1007/s10562-011-0579-1.
[11] O. Al, J. Lin, C. Ma, Q. Wang, Y. Xu, G. Ma, J. Wang, Enhanced low-temperature performance of CO_2 methanation over, Appl. Catal. B Environ. 243 (2019) 262–272, doi:10.1016/j.apcatb.2018.10.059.
[12] W. Keen, M. Tahir, Structured clay minerals-based nanomaterials for sustainable photo /thermal carbon dioxide conversion to cleaner fuels : a critical review, Sci. Total Environ. 845 (2022) 157206, doi:10.1016/j.scitotenv.2022.157206.
[13] C.E. Daza, A. Kiennemann, S. Moreno, R. Molina, Dry reforming of methane using Ni–Ce catalysts supported on a modified mineral clay, Appl. Catal. A Gen. 364 (2009) 65–74, doi:10.1016/j.apcata.2009.05.029.
[14] C. Daza, A. Kiennemann, S. Moreno, R. Molina, Stability of Ni-Ce catalysts supported over Al-PVA modified mineral clay in dry reforming of methane, Energy Fuels 23 (2009) 3497–3509, doi:10.1021/ef9000874.
[15] O.H. Ojeda-Niño, F. Gracia, C. Daza, Role of Pr on Ni–Mg–Al mixed oxides synthesized by microwave-assisted self-combustion for dry reforming of methane, Ind. Eng. Chem. Res. (2019) 7909–7921, doi:10.1021/acs.iecr.9b00557.
[16] M.N. Timofeeva, S.T. Khankhasaeva, Y.A. Chesalov, S.V Tsybulya, Synthesis of Fe, Al-pillared clays starting from the Al, Fe-polymeric precursor : effect of synthesis parameters on textural and catalytic properties, Appl. Catal. B Environ. Environ. 88 (2009) 127–134, doi:10.1016/j.apcatb.2008.09.013.
[17] A. Milutinovic, A. Nastasovic, D. Lonc, I. Vukovic, K. Loos, Z. Vukovic, D. Jovanovic, Textural properties of poly(glycidyl methacrylate): acid-modified bentonite nanocomposites, Polym. Bull. (2013) 1805–1818, doi:10.1007/s00289-013-0924-1.
[18] A. Gil, S.A. Korili, R. Trujillano, M. Angel, A review on characterization of pillared clays by specific techniques, Appl. Clay Sci. 53 (2011) 97–105, doi:10.1016/j.clay.2010.09.018.
[19] X. Yang, M. Huang, H. Huang, D. Li, Y. Zhan, L. Jiang, Carbon dioxide methanation over Ni catalysts prepared by reduction of $Ni_xMg_{3-x}Al$ hydrotalcite-like compounds: Influence of Ni:Mg molar ratio, Int. J. Hydrog. Energy. 47 (2022) 22442–22453, doi:10.1016/j.ijhydene.2022.05.076.
[20] J. Ren, C. Mebrahtu, R. Palkovits, Ni-based catalysts supported on Mg-Al hydrotalcites with different morphologies for CO_2 methanation: exploring the effect of metal-support interaction, Catal. Sci. Technol. 10 (2020) 1902–1913, doi:10.1039/c9cy02523e.
[21] Y. Li, Y. Wang, X. Zhang, X. Ding, Z. Liu, R. Zhu, L. Wu, L. Zheng, Ni supported on natural clay of palygorskite as catalyst for dry reforming of methane: thermodynamic analysis and impacts of preparation methods, Int. J. Hydrog. Energy. 47 (2022) 20851–20866, doi:10.1016/j.ijhydene.2022.04.195.
[22] S.I. Fujita, B.M. Bhanage, D. Aoki, Y. Ochiai, N. Iwasa, M. Arai, Mesoporous smectites incorporated with alkali metal cations as solid base catalysts, Appl. Catal. A Gen. 313 (2006) 151–159, doi:10.1016/j.apcata.2006.07.018.
[23] H. Lu, X. Yang, G. Gao, K. Wang, Q. Shi, J. Wang, C. Han, J. Liu, M. Tong, Mesoporous zirconia-modified clays supported nickel catalysts for CO and CO_2 methanation, Int. J. Hydrog. Energy. 39 (2014) 18894–18907, doi:10.1016/j.ijhydene.2014.09.076.
[24] F. Mérimé, B. Kontchouo, Z. Gao, Methanation of CO_2 over Ni /clay : effects of calcination temperature on catalyst properties and reaction intermediates formed, Int. J. Energy Res. (2022) 1–15, doi:10.1002/er.8521.
[25] Y. Jiang, T. Huang, L. Dong, Z. Qin, H. Ji, Engineering Ni/bentonite catalysts prepared by solution combustion method for CO2 methanation ☆, Chin. J. Chem. Eng. 26 (2018) 2361–2367, doi:10.1016/j.cjche.2018.03.029.
[26] Y. Jiang, T. Huang, L. Dong, T. Su, B. Li, X. Luo, X. Xie, Z. Qin, C. Xu, H. Ji, Mn Modified Ni/Bentonite for CO_2 Methanation, Catalysts (2018), doi:10.3390/catal8120646.
[27] C. Liang, Z. Gao, H. Lian, X. Li, S. Zhang, ScienceDirect impacts of metal loading in Ni /attapulgite on distribution of the alkalinity sites and reaction intermediates in CO_2 methanation reaction, Int. J. Hydrog. Energy. 45 (2020) 16153–16160, doi:10.1016/j.ijhydene.2020.04.070.
[28] H.U. Hambali, A.A. Jalil, A.A. Abdulrasheed, T.J. Siang, Y. Gambo, A.A. Umar, Zeolite and clay based catalysts for CO_2 reforming of methane to syngas: a review, Int. J. Hydrog. Energy. 47 (2022) 30759–30787, doi:10.1016/j.ijhydene.2021.12.214.